Cell Calcium (1992) 13, 391–400

Solution structure of calmodulin and its complex with a myosin light chain kinase fragment

M. IKURA[1*], G. BARBATO[1**], C.B. KLEE[2] and A. BAX[1]

[1] *Laboratory of Chemical Physics, National Institute of Diabetes and Digestive and Kidney Diseases, National Institutes of Health, Bethesda, Maryland, USA*
[2] *Laboratory of Biochemistry, National Cancer Institute, National Institutes of Health, Bethesda, Maryland, USA*

Abstract — The solution structure of Ca^{2+} ligated calmodulin and of its complex with a 26-residue peptide fragment of skeletal muscle myosin light chain kinase (skMLCK) have been investigated by multi-dimensional NMR. In the absence of peptide, the two globular domains of calmodulin adopt the same structure as observed in the crystalline form [2]. The so-called 'central helix' which is observed in the crystalline state is disrupted in solution. ^{15}N relaxation studies show that residues Asp78 through Ser81, located near the middle of this 'central helix', form a very flexible link between the two globular domains. In the presence of skMLCK target peptide, the peptide-protein complex adopts a globular ellipsoidal shape. The helical peptide is located in a hydrophobic channel that goes through the center of the complex and makes an angle of ~45° with the long axis of the ellipsoid.

Calmodulin (CaM) is a ubiquitous intracellular protein of 148 residues (M_r 16.7 kD) that plays a key role in coupling Ca^{2+} transients caused by a stimulus of the cell surface to events in the cytosol [1]. It performs this role by calcium dependent binding to a host of intracellular enzymes. The crystal structure of calmodulin shows a highly unusual dumbbell type shape, where two globular domains (each containing two calcium binding sites) are connected by a 25-residue long α-helix [2, 3]. This so-called 'central helix', which actually shows significant distortions near its middle in the crystalline state [2], has been the subject of much debate. For example, small angle X-ray scattering studies were interpreted by different workers to confirm the presence of a rigid 'central helix' in solution [4] and as evidence that the 'central helix' must be bent or highly flexible [5].

The present paper discusses the results of a study of CaM in solution by nuclear magnetic resonance (NMR) techniques. The detailed NMR characterization of proteins with the complexity of CaM has

Present addresses:
*Division of Molecular and Structural Biology, Ontario Cancer Institute, 500 Sherbourne Street, Toronto, Ontario, Canada M4X 1K9
**Istituto di Recerca di Biologia Molecolare, via Pontina, km 30,600, Pomezia, Rome, Italy

become feasible only very recently by the introduction of advanced NMR methodology. This new methodology, largely developed using CaM as a test protein [6], relies on the incorporation of the stable isotopes ^{13}C and ^{15}N in the protein. The NMR spectra of such a uniformly isotopically enriched protein can be separated in three or four orthogonal frequency dimensions, thereby greatly decreasing resonance overlap and facilitating spectral interpretation [6–8]. In addition, these stable isotopes provide very direct access to the study of internal protein mobility and thus enable the detailed characterization of both the structure and the dynamics of the CaM 'central helix'.

Materials and Methods

Recombinant *Drosophila* CaM was prepared using *Escherichia coli* (strain AR58) harboring the pAS expression vector [9]. Uniform labeling with ^{13}C and ^{15}N at levels of more than 95% was obtained by growing the bacteria in M9 minimal media with [^{15}N]-NH_4Cl (1 g/l) and [$^{13}C_6$]-glucose (3 g/l) as the sole nitrogen and carbon sources, respectively. A 2.5 l cell culture yielded ~20 mg purified CaM. The 26-residue unlabeled synthetic peptide comprising the CaM binding domain (residues 577–602) of skeletal muscle myosin light chain kinase, commonly referred to as M13 [10], was purchased from Peptide Technologies (Washington, DC, USA) and used without further purification. Sample preparations contained 1–1.5 mM CaM, 4.5–6.5 mM Ca^{2+}, 100 mM KCl, pH 6.3–6.8, and one molar equivalent of M13 peptide for studies of the M13–CaM complex. All experiments were conducted at 35°C.

^{15}N NMR relaxation experiments were carried out on a modified Bruker AM-500 spectrometer. Details regarding the experimental set-up are presented elsewhere [11, 12]. Experiments for determination of the 3D structure of the CaM–M13 complex were conducted both at 500 MHz ^1H frequency on the above mentioned Bruker AM-500 spectrometer and on a Bruker AMX-600 spectrometer, operating at 600 MHz ^1H frequency, and equipped with Bruker hardware for carrying out the required triple resonance experiments.

Results and Discussion

Structure of the CaM 'central helix'

During the assignment process [13] of CaM, it became clear from the observed NOE patterns that for residues in the two globular domains (residues T5 through R74 and E83 through T146) of CaM the solution structure is very close to that previously observed in the crystalline state [2, 3]. Because of the large amount of labor required for determining a high resolution NMR structure, the solution structure of each of the individual domains was not redetermined. Instead, our NMR investigation has focused mainly on a detailed characterization of the 'central helix' in CaM.

The main NMR indicators for α-helical structure in proteins are the characteristic short distances [14] between the amide protons of adjacent residues, between the Cα proton of residue *i* and the amide proton of residue *i*+3, and between the Cα proton of residue *i* and the Cβ proton of residue *i*+3. These short distances give rise to so-called $d_{NN}(i,i+1)$, $d_{\alpha N}(i,i+3)$ and $d_{\alpha\beta}(i,i+3)$ NOE connectivities. The $d_{\alpha N}(i,i+1)$ NOE is weak in an α-helix because of the relatively long distance between the Cα proton of residue *i*, and the amide of residue *i*+1 [14]. A string of adjacent residues with small values (≤6 Hz) for the J coupling, $^3J_{HNH\alpha}$, between the amide and the Cα proton and positive secondary chemical shifts for the $^{13}C\alpha$ resonances ($\Delta^{13}C\alpha$) [15, 16] are additional indicators for α-helical structure. Finally, hydrogen bonded amides in an α-helix are expected to exchange relatively slowly with solvent because the exchange event requires breaking of the hydrogen bond.

Figure 1 summarizes the above mentioned parameters for the central helix in CaM. As can be seen from this figure, the residues at the beginning (E66–K77) and end (E82–F92) of the 'central helix' show the signatures of α-helical conformation. However, from D78 through S81, the conformation is clearly not helical, based on the strong $d_{\alpha N}(i,i+1)$ and absent $d_{NN}(i,i+1)$ NOEs, rapid hydrogen exchange, and near-zero values for the secondary Cα and Cβ (not shown) shifts. These observations for D78–S81 are most compatible with an unstructured 'random coil' conformation for these

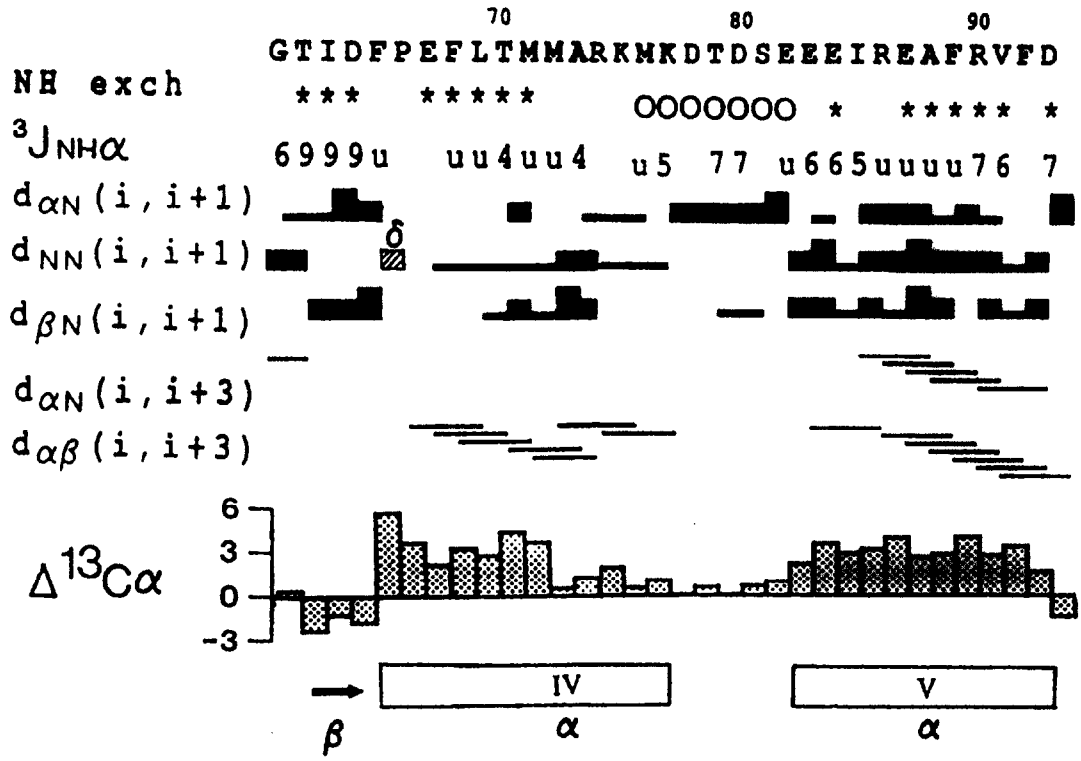

Fig. 1 Summary of the NMR parameters measured for residues G61–D93 in Ca^{2+}-saturated CaM. Amide protons that exchange faster than 10 s^{-1} at pH 7, 35°C, are marked by open circles. Asterisks mark amide protons that are not fully exchanged 10 min after the protein is dissolved in D_2O at 25°C, pH 6.75. The three-bond $J_{HNH\alpha}$ couplings are indicated by numbers. Couplings marked 'u' are unresolved, (≤5 Hz). The $d_{\alpha N}$, $d_{\beta N}$ and d_{NN} NOE connectivities are marked by horizontal bars with a thickness determined by the NOE intensity. The $d_{\alpha N}(i,i+3)$ and $d_{\beta N}(i,i+3)$ lines indicate an observed NOE connectivity. In addition to the $d_{\alpha N}(i,i+3)$ connectivities marked, $d_{\alpha N}(i,i+3)$ was also observed for E67/T70, F68/M71, L69/M72 and T70/A73, but these connectivities were accidently omitted from the figure. The bar graph marked $\Delta^{13}C_\alpha$ shows the secondary C_α chemical shift. The bottom of the figure delineates the secondary structure, determined on the basis of NOE, J coupling, and secondary C_α chemical shift patterns. Adapted from [13]

residues. Note, however, that the exact location where the helix transforms into a 'random coil' is not clearly defined as, for example, secondary C_α shifts for K75 and M76 are already smaller than expected for an α-helix and the amide proton exchange rate gradually increases for residues K75–D78 [17]. The beginning of the second half of the 'central helix' at E82 is defined much more sharply by a clear transition in the NOE pattern from intense $d_{\alpha N}(i,i+1)$ NOEs to intense $d_{NN}(i,i+1)$ NOEs, a relatively sharp increase in secondary C_α chemical shift, and a sharp decrease in hydrogen exchange rate.

Dynamics of CaM

The findings mentioned above are strongly indicative of a 'flexible hinge' type connection, formed by residues D78–S81, between the two globular CaM domains. However, the degree of flexibility cannot be quantified on the basis of the parameters reported in Figure 1. In proteins which are isotopically enriched with ^{15}N, a detailed characterization of the protein backbone dynamics can be accomplished in a straightforward manner by ^{15}N relaxation measurements [18]. A detailed discussion of the relaxation mechanisms falls

beyond the scope of this article and only a brief qualitative discussion of the salient points will be presented. Three different ^{15}N relaxation parameters are of most practical importance for characterizing its dynamics: the longitudinal relaxation time, T_1, the transverse relaxation time, T_2, and the ^{15}N-{^1H} heteronuclear NOE. It is important to realize that all these relaxation processes are dominated by the ^1H-^{15}N magnetic dipole-dipole interaction. Therefore, it is the time dependence of the orientation of each NH bond vector in the protein which determines the relaxation properties of a given ^{15}N nucleus.

The T_1 relaxation time is the time constant for the ^{15}N magnetization to return to its equilibrium value. This relaxation involves a large change in energy to flip nuclei that are oriented antiparallel to the magnetic field into a parallel orientation. The T_1 relaxation process is most efficient for NH bond vectors that reorient with a characteristic rotational correlation time τ_c, equal to $1/(\omega_N)$, where ω_N is the angular ^{15}N resonance frequency, expressed in radians per second (2π x 50.7 MHz in our experiments). Thus, T_1 relaxation is most rapid for a correlation time τ_c ~3 ns. In macromolecules, the transverse relaxation time, T_2, is dominated by 'incomplete averaging' of the ^1H-^{15}N dipolar interaction. The instantaneous ^{15}N resonance frequency depends on the size of the truncated ^{15}N-^1H dipolar interaction, i.e. on the orientation of the NH bond vector with respect to the static magnetic field. Rapid random reorientation of the molecule averages this time dependent dipolar contribution to the ^{15}N resonance frequency to zero. However, if reorientation of the molecule is not infinitely fast, the incomplete averaging results in a rapid decay of ^{15}N transverse magnetization. Therefore, transverse relaxation times monotonically decrease with increasing correlation time, τ_c. Finally, the ^{15}N-{^1H} NOE represents the ratio of the value of the ^{15}N magnetization in thermal equilibrium in the presence and absence of saturation of the ^1H transitions. For correlation times longer than ~3 ns, the NOE is close to a limiting value of ~0.8. For $\tau_c < 0.1$ ns, the NOE has a value of ~ –3.5.

Above, it has been assumed that the protein reorients as a rigid body. However, in practice the relaxation is influenced substantially by internal motions that occur on a time scale, τ_e. The effect of such internal motions is most easily analyzed using the model-free approach developed by Lipari and Szabo [19]. In this approach, a mixture of the spectral density function, $J(\omega)$, associated with the slow overall molecular tumbling, $J_s(\omega)$, and the spectral density caused by the fast internal motions, $J_{int}(\omega)$, is assumed:

$$J(\omega) = S^2 J_s(\omega) + (1 - S^2) J_{int}(\omega) \quad \ldots . \text{Eq. 1}$$

where $J_s(\omega) = \tau_c/[1 + (\omega\tau_c)^2]$ and $J_{int}(\omega) = \tau/[1 + (\omega\tau)^2]$, with $1/\tau = 1/\tau_e + 1/\tau_c$, τ_e being the time scale of the internal motions. The degree of internal flexibility is thus described by the generalized order parameter S^2. This approach for the simultaneous analysis of both the reorientation of the entire protein and its internal dynamics is valid indep- endent of the type of internal motion. If, for example, the internal motions are described by free diffusion in a cone with semiangle α, the general- ized order parameter is related to α according to:

$$S^2 = [\cos\alpha\,(1 + \cos\alpha)/2]^2 \quad \ldots . \text{Eq. 2}$$

The ^1H-{^{15}N} NOE and the T_1 and T_2 relaxation times have been measured for 114 backbone amides in CaM which show non- overlapping resonances in the ^{15}N-^1H shift correlation spectrum. The results are summarized in Figure 2 (panels a–c).

For amides with an NOE > ~0.6, the correlation time, τ_c, with which an individual bond vector reorients can be calculated from the T_1/T_2 ratio [18]. These τ_c values are shown in Figure 2d. As can be seen, the τ_c values are remarkably similar to one another within each of the two domains, the small degree of variation in τ_c is mainly caused by random measurement error. The closeness of the τ_c values indicates that the individual domains reorient nearly isotropically. If calmodulin were tumbling as a rigid dumbbell, hydrodynamic calculations show that the apparent correlation times derived from the T_1/T_2 ratios would be 1.5 times longer for NH bond vectors parallel to the long dumbbell axis compared to NH bond vectors perpendicular to this axis [12]. In fact, it is interesting to note that the average

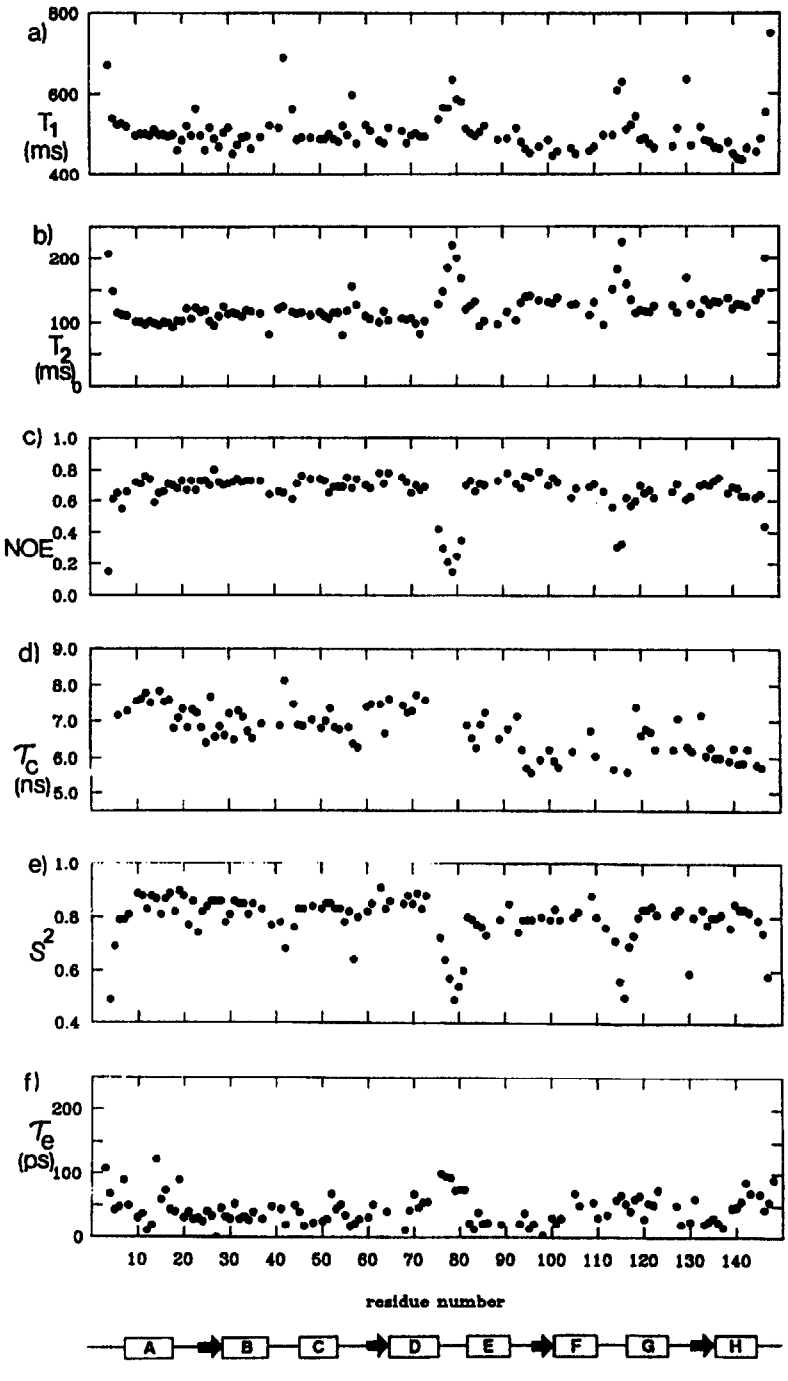

Fig. 2 Plots as a function of residue number in free Ca^{2+}-saturated CaM of the measured (a) T_1, (b) T_2, and (c) ^{15}N-{^1H} NOE: (d) the apparent correlation time, τ_e, derived from the T_1/T_2 ratio, (e) the generalized order parameter S^2, and (f) the correlation time for fast internal motions. From [12]

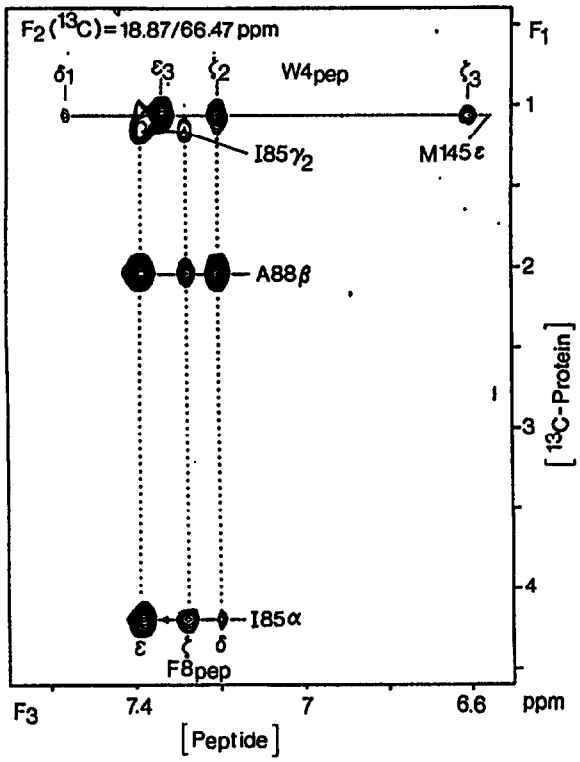

Fig. 3 Small region of a cross section taken through the 3D ^{13}C (F_2)-separated ^{13}C (F_3)-filtered NOESY spectrum of the CaM–M13 complex. This spectrum displays exclusively intermolecular NOE connectivities between protons attached to ^{13}C (i.e. CaM protons) in the F_1 dimension, and protons attached to ^{12}C (i.e. M13 protons) in the F_3 dimension. The slice has been taken at a F_2 frequency which selects CaM protons attached to carbons resonating at 18.87+Nx23.8 ppm (N = 0,1,2,...). From [21]

correlation time of residues in the C-terminal domain is somewhat shorter than in the N-terminal domain, as would be expected for a larger body (the N-terminal domain) connected to a smaller rigid body (the C-terminal domain) via a flexible linker (D78–S81).

The ^{15}N relaxation results provide another independent method for defining the exact location of the flexible hinge in the 'central helix'. As can be seen from Figure 2e, the order parameters for the individual bond vectors along the backbone of the individual CaM domains are quite uniform, except for low order parameters (i.e. high internal mobility) in the loops connecting helices B and C and helices F and G. Within the 'central helix', the generalized order parameter S^2 is very close to its regular value of 0.85 up till residue A73. No accurate relaxation times could be measured for R74 and K75 because of partial resonance overlap. However, from M76 (S^2 = 0.72) through T79 (S^2 = 0.49) the order parameters steadily decrease. Order parameters remain low for D80 (0.54) and S81 (0.60) and are back to a value that is compatible with a rigid structure at E82 (S^2 = 0.80).

The ^{15}N relaxation study quantitates the degree of flexibility in the 'central helix' and finds the increase in flexibility to be most pronounced for residues D78–S81 ($S^2 \leq 0.6$), exactly the same residues that were implicated to be in a 'random coil' conformation based on the NMR parameters shown in Figure 1. The ^{15}N relaxation experiments show that: (a) the correlation times for the N-terminal and C-terminal domains are different and proportional to the size of the domain; (b) the correlation times for the individual amide bond vectors vary to a much lesser degree than predicted by hydrodynamic calculations for rigid dumbbell models; and (c) the order parameters for residues near the middle of the 'central helix' are low. These findings strongly support the 'flexible tether hypothesis', where the central helix serves merely to keep the two domains in close proximity for binding to their target. As will be discussed below, this high degree of flexibility is indeed essential for CaM binding to the M13 peptide.

Structure of the CaM–M13 complex

Ca^{2+}-saturated CaM has a high affinity (~10^{-9} M) for a 26 residue peptide, known as M13, which comprises residues 577–602 of skeletal muscle myosin light chain kinase [10]. This peptide and many others that exhibit a high affinity for CaM are positively charged and have the propensity for α-helix formation [20]. Indeed, circular dichroism studies of CaM complexed with M13 have shown an increase in α-helicity for the complex compared to Ca^{2+}-saturated CaM alone, suggesting that the peptide adopts an α-helical conformation in its complex with CaM. However, because of the

difficulty of growing X-ray suitable crystals of the CaM–M13 complex, no crystal structure for the complex has been reported. We have succeeded, however, in determining its structure in solution [21], using NMR techniques. Below, the salient points of this work will be briefly discussed.

Two different approaches can be taken to determine the peptide conformation in the CaM–M13 complex. First, if the peptide is isotopically enriched with ^{15}N and/or ^{13}C, the new isotope directed 3D NMR methods can be used to selectively highlight the signals of protons attached to these enriched $^{15}N/^{13}C$ nuclei. Uniform isotopic enrichment of synthetic peptides is prohibitively expensive, however. A compromise approach, enriching only the backbone amides of the 'cheap' amino acids in the peptide representing the CaM-binding domain smooth muscle MLCK was taken by Roth et al. [22] and these workers indeed found the peptide to be in an α-helical conformation, albeit with a distinct kink near its middle. We have taken a different approach: by using unlabeled peptide and uniformly ^{15}N and ^{13}C enriched CaM, it was possible to select only signals from those protons that are not attached to ^{13}C or ^{15}N, reducing the spectral complexity to that of the peptide alone. This study of the M13 peptide showed it to be α-helical from residue R3 through S21, with a substantial degree of mobility for its five C-terminal residues [23].

The next stage of the structural study of the complex involves the determination of peptide-protein NOEs. Using the fact that the peptide is unlabeled, whereas CaM is enriched uniformly with ^{15}N and ^{13}C, the most straightforward NMR approach for identification of intermolecular NOEs involves filtering of the signals in such a way that only NOE interactions between a ^{12}C- and a ^{13}C-attached proton are observed. In order to reduce spectral overlap and to facilitate spectral assignment, these ^{1}H–^{1}H interactions are separated into a third dimension (the chemical shift of the ^{13}C attached to the CaM proton). An example of several important interactions observed in this manner is shown in Figure 3, which displays NOEs between the C_ε methyl protons of CaM Met-145 and the ring protons of peptide residue W4. This same region of the 3D spectrum shows NOEs between the ring protons of peptide residue F8 and CaM residues A88 and I85, located in the C-terminal half of the 'central helix'.

Figure 4 summarizes all the intermolecular NOEs observed for the CaM–M13 complex. Most of these interactions involve hydrophobic residues. Of particular importance appear to be the numerous NOE interactions between peptide residue W4 and a cluster of hydrophobic residues in the C-terminal domain, and between peptide residue F17 and a cluster of hydrophobic residues in the N-terminal domain. Sequence analysis of a substantial number of peptides with high affinity for CaM shows that two hydrophobic residues, separated by a stretch of 12 residues, constitute a common feature of these peptides, suggesting that they all interact with CaM in a similar manner [21].

As shown in Figure 4, a number of peptide residues show NOEs to both the N- and C-terminal domains of CaM. Particularly interesting are the NOEs observed between peptide residue S12 and CaM residues M72 and A88, both located in the 'central helix'. Clearly the NOEs observed between M13 and CaM are incompatible with the structure observed for CaM in the crystalline state (in the absence of M13). Although the M13–CaM NOEs would be sufficient for model building of the complex, using the assumption that the two globular domains do not change their structure, we decided to go ahead and determine the structure of the entire complex instead. This involves the additional analysis of a very large number of NOEs within CaM, which determine the structure of the individual domains. In the first rounds of analysis of the NOE spectrum, 1490 such NOEs have been identified. Although this number of distances, even when supplemented by 133 intermolecular NOEs and 164 intramolecular M13 NOEs, is quite small for a 20 kD complex, it is sufficient to build a medium resolution structure. A total of 24 such structures were calculated. A ribbon diagram displaying the backbone conformation of the complex is shown in Figure 5. Particularly striking is the high degree of symmetry of the complex in this particular view. A more detailed discussion and additional views of this complex have been presented elsewhere [21].

When only considering CaM residues 6–73 and

83–146, the atomic root-mean-square (rms) distribution about the mean coordinate position for the 24 calculated structures is 1.4 Å. The conformation of residues R74–E82 is poorly determined by the NMR data because of a lack of long range NOEs for these residues. These 'central helix' residues are part of a flexible and solvent exposed loop that surrounds the peptide (Fig. 5). Rapid exchange rates for the amide protons of CaM residues K75–E82 [17] confirm this finding.

Conclusions

Dramatic advances in NMR methodology that have occurred during the last 5 years have made it possible to obtain a detailed picture of the structure and dynamics of proteins such as CaM and its complex with M13. This NMR work settles the dispute about the solution conformation of the CaM 'central helix' and clearly shows that the middle of this 'central helix' adopts a highly flexible structure, which in no respect resembles an α-helix. CaM, therefore, is a clear example where studies of the structure in solution, using NMR, and in the crystalline state, using X-ray crystallography, offer a quite different view.

The flexible nature of the 'central helix' is essential for binding its target peptides in the manner illustrated in Figure 5, as the middle of this 'central helix' has to bend around the α-helical peptide. Qualitatively, this structure of the complex resembles that of the class III model for the complex, proposed by Persechini and Kretsinger [24]. The general features of this model and the NMR-based structure, namely the two domains

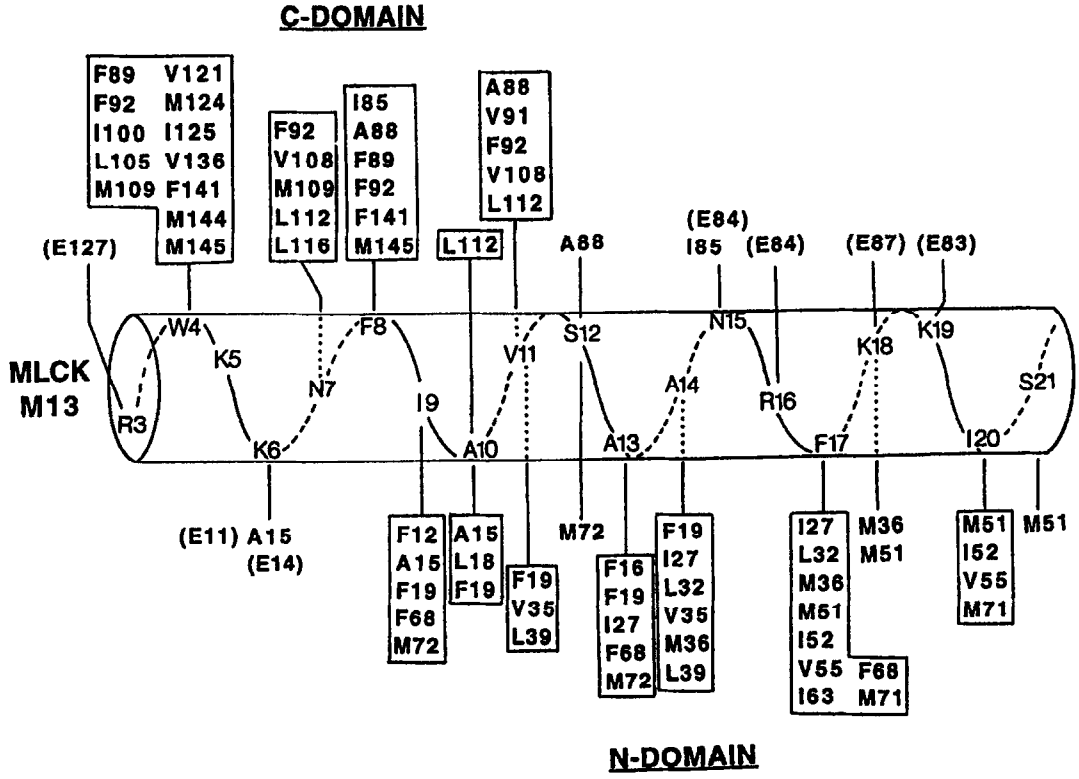

Fig. 4 Summary of residue pairs for which intermolecular NOEs between CaM and M13 are observed. CaM residues involved in hydrophobic interactions are boxed. Also included are potential electrostatic interactions between negatively charged CaM glutamates, shown in parentheses, and positively charged lysine and arginine residues of M13. Note that these electrostatic interactions have been inferred solely from the structure as no NOEs have as yet been identified between these pairs of residues. From [21]

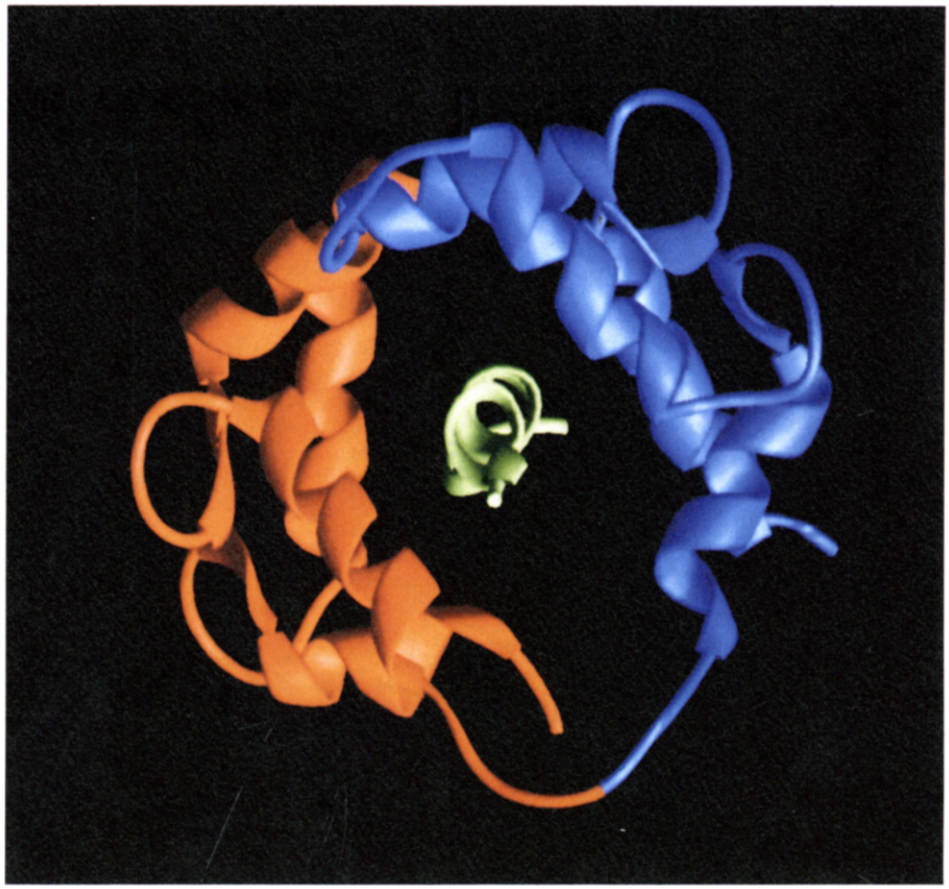

Fig. 5 Ribbon diagram representation of the CaM–M13 complex, viewed parallel to the helical M13 peptide (green). The CaM N-terminal domain is shown in blue, the C-terminal domain in red. Adapted from [21]

coming in close proximity to form a hydrophobic channel occupied by an α-helical peptide, are similar in the two cases. The main differences relate to the reverse orientation of the peptide, and the relative positioning of the two CaM domains. This latter difference results from the constraint used in the modelling study to leave the X-ray crystal structure as intact as possible, and permitting only the backbone angles of residue S81 to vary. As a result, when the carboxy-terminal domain of the model and of our NMR structure are superimposed, the amino-terminal domains show an rms displacement of ~8 Å.

The structure calculated for the CaM–M13 complex is of much lower precision than what is obtainable from a more detailed spectral analysis [25]. For example, no stereospecific assignments of Cβ methylene protons or of the methyl groups of valine and leucine residues have been used so far. Also, a large number of long range NOEs, particularly in crowded spectral regions, have not yet been identified. It is anticipated that a more detailed study of the CaM–M13 complex, using these additional structural parameters, will yield a structure with a precision that is similar to that obtained for the protein interleukin-1β, which has been considered comparable in resolution to a ~2 Å crystal structure [25].

Acknowledgements

We thank Kathy Beckingham and John F. Maune for providing us with the *Drosophila* calmodulin coding

construct, Marius Clore and Angela Gronenborn for stimulating discussions, Rolf Tschudin for making the necessary hardware modifications and Dennis Torchia for continuous advice and for use of his modified AM500 spectrometer. Lewis Kay and Sylvia Spera conducted several of the experiments on CaM and the CaM–M13 complex. This work was supported by the Intramural AIDS Anti-viral Program of the Office of the Director of the National Institutes of Health.

References

1. Cohen P. Klee CB. (eds) (1988) Molecular Aspects of Cellular Regulaition. Vol. 5. New York, Elsevier.
2. Babu YS. Bugg CE. Cook WJ. (1988) Structure of calmodulin refined at 2.2 Å resolution. J. Mol. Biol., 204, 191-204.
3. Taylor DA. Sack JS. Maune JF. Beckingham K. Quiocho FA. (1991) Structure of recombinant calmodulin from *Drosophila melanogaster* refined at 2.2-Å resolution. J. Biol. Chem., 266, 21375-21380.
4. Seaton BA. Head JGF. Engelman DM. Richards FM. (1985) Calcium-induced increase in the radius of gyration and maximum dimension of calmodulin measured by small-angle X-ray scattering. Biochemistry, 24, 6740-6743.
5. Heidorn DB. Trewhella J. (1988) Comparison of the crystal and solution structures of calmodulin and troponin C. Biochemistry, 27, 909-915.
6. Ikura M. Kay LE. Bax A. (1990) A novel approach for sequential assignment of ^{1}H, ^{13}C, and ^{15}N spectra of larger proteins: Heteronuclear triple-resonance three-dimensional NMR spectroscopy. Application to calmodulin. Biochemistry, 29, 4659-4667.
7. Fesik SW. Zuiderweg ERP. (1988) Heteronuclear three-dimensional NMR spectroscopy. A strategy for the simplification of homonuclear two-dimensional NMR spectra. J. Magn. Reson., 78, 588-593.
8. Kay LE. Clore GM. Bax A. Gronenborn AM. (1990) Four-dimensional heteronuclear triple-resonance NMR spectroscopy of interleukin-1β in solution. Science, 249, 411-414.
9. Shatzman AR. Rosenberg M. (1985) Efficient expression of heterologous genes in *Escherichia coli*. Ann. NY Acad. Sci., 478, 233-248.
10. Klevit RE. Blumenthal DK. Wemmer DE. Krebs J. (1985) Interaction of calmodulin and a calmodulin-binding peptide from myosin light chain kinase. Major spectral changes in both occur as the result of complex formation. Biochemistry, 24, 8152-8157.
11. Kay LE. Nicholson LK. Delaglio F. Bax A. Torchia DA. (1992) Pulse sequences for removal of the effects of cross correlation between dipolar and chemical-shift anisotropy relaxation mechanisms on the measurement of heteronuclear T_1 and T_2 values in proteins. J. Magn. Reson., 97, 359-375.
12. Barbato G. Ikura M. Kay LE. Pastor RW. Bax A. (1992) Backbone dynamics of calmodulin studied by ^{15}N relaxation using inverse detected two-dimensional NMR spectroscopy: The central helix is flexible. Biochemistry, In press.
13. Ikura M. Spera S. Barbato G. Kay LE. Krinks M. Bax A. (1991) Secondary structure and side chain ^{1}H and ^{13}C resonance assignments of calmodulin in solution by heteronuclear multidimensional NMR spectroscopy. Biochemistry, 30, 9216-9228.
14. Wüthrich K. (1986) NMR of Proteins and Nucleic Acids. New York, Wiley.
15. Spera S. Bax A. (1991) Empirical correlation between protein backbone conformation and C_α and C_β ^{13}C nuclear magnetic resonance chemical shifts. J. Am. Chem. Soc., 113, 5490-5492.
16. Wishart DS. Sykes BD. Richards FM. (1991) Relationship between nuclear magnetic resonance chemical shift and protein secondary structure. J. Mol. Biol., 222, 311-333.
17. Spera S. Ikura M. Bax A. (1991) Measurement of the exchange rates of rapidly exchanging amide protons: Application to the study of calmodulin and its complex with a myosin light chain kinase fragment. J. Biomol. NMR, 1, 155-165.
18. Kay LE. Torchia DA. Bax A. (1989) Backbone dynamics of proteins as studied by ^{15}N inverse detected heteronuclear NMR spectroscopy. Application to Staphylococcal nuclease. Biochemistry, 28, 8972-8979.
19. Lipari G. Szabo A. (1982) Model-free approach to the interpretation of nuclear magnetic resonance relaxation in macromolecules. 1. Theory and range of validity. 2. Analysis of experimental results. J. Am. Chem. Soc., 104, 4546-4570.
20. Blumenthal DK. Krebs EG. (1988) Calmodulin-binding domains on target proteins. In: Cohen P. Klee CB. (eds). Molecular Aspects of Cellular Regulation, vol. 5. New York, Elsevier, pp. 341-356.
21. Ikura M. Clore GM. Gronenborn AM. Zhu G. Klee CB. Bax A. (1992) Solution structure of a calmodulin-target peptide complex by multidimensional NMR. Science, 256, 632-638.
22. Roth SM. Schneider DM. Strobel LA. VanBerkum MFA. Means AR. Wand AJ. (1991) Structure of the smooth muscle myosin light-chain kinase calmodulin-binding domain peptide bound to calmodulin. Biochemistry, 30, 10078-10084.
23. Ikura M. Bax A. (1992) Isotope filtered 2D NMR of a protein-peptide complex. Study of a skeletal muscle myosin light chain kinase fragment bound to calmodulin. J. Am. Chem. Soc., 114, 2433-2440.
24. Persechini A. Kretsinger RH. (1988) Toward a model of the calmodulin-myosin light chain kinase complex: Implications for calmodulin function. J. Cardiovasc. Pharmacol., 12 Suppl 5, 1-12.
25. Clore GM. Wingfield PT. Gronenborn AM. (1991) High-resolution three-dimensional structure of interleukin 1β in solution by three- and four-dimensional nuclear magnetic resonance spectroscopy. Biochemistry, 30, 2315-2323.

Please send reprint requests to : Dr Ad Bax, Laboratory of Chemical Physics, National Institute of Diabetes and Digestive and Kidney Diseases, National Institutes of Health, Bethesda MD 20892, USA